CHAPTER 1

MATERIAL MODELING WITH IMPEDANCE MATCHING

To get an idea of how a binder material behaves under shock loading, there are several experiments that can be performed. Here, a series of reverb experiments were performed on the UV resin. Reverb experiments are effective at determining equation of state data for low impedance materials such as polymers. Equation of state information can be calculated from experimental results using the method of impedance matching, whereby pressure-particle velocity points can be determined for one Hugoniot state and for one or more release states. Conventionally, impedance matching requires the assumption that the yield strength of the material is insignificant in comparison to the pressures achieved; however, at low velocities this assumption may be imprecise, and the elastic behavior of the material must be considered. Considering the elastic behavior of the material makes the impedance matching method not straightforward as will be discussed.

1.1 Theory of Impedance Matching

Impedance matching is a convenient method of determining the pressure and particle velocity of a shock wave after an interaction when both material models are known [1]; furthermore, if one material model is not known, but the resulting particle velocity is known, the method of impedance matching can be reversed to determine information about the unknown material model. Impedance matching requires little more than the conservations of mass (Equation 1.1) and momentum (Equation 1.3) as well as some understanding of the physics of shock waves.

The conservation equations are derived from a control volume that moves with the shock front, as illustrated in Figure 1.1. This control volume can be viewed from two reference frames: the Eulerian reference frame, where the reference frame

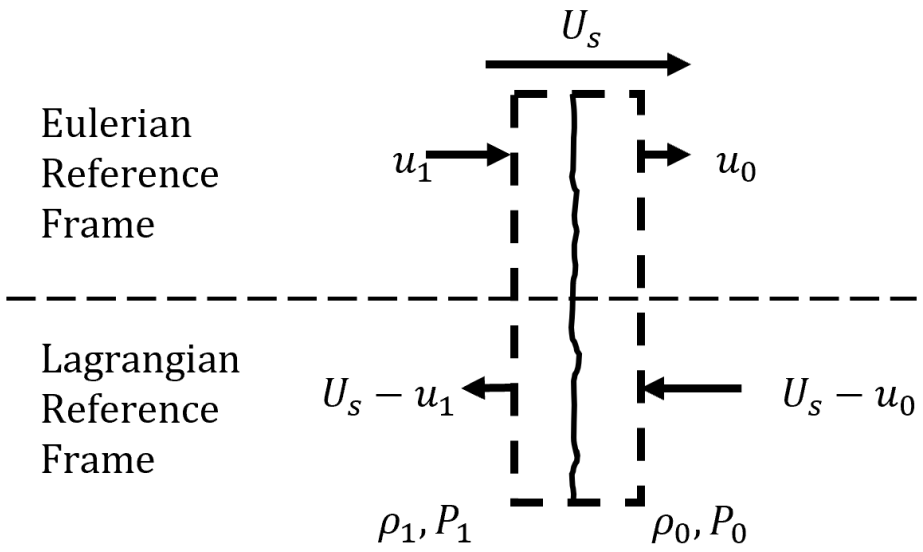

Figure 1.1: Shock front control volume.

is fixed and the control volume moves through space, or the Lagrangian reference frame, which moves with the shock wave, and the control volume is fixed with respect to the reference frame. It will be assumed that flow of material through the control volume is steady, resulting in a constant shock velocity. Therefore the two frames can be related by the Galilean transformation $\dot{x}' = \dot{x} + C$ (where C is the shock velocity[1] and $\dot{x}$ is the velocity of some particle in the lab frame and $\dot{x}'$ is the velocity of the same particle in a frame moving with the shock); given that neither frame is accelerating, an observer moving with either frame would see different phenomena. According to Galilean relativity, the phenomena apparent to each observer must follow the laws of physics, such as conservations of mass, momentum, and energy [3][4]. Therefore, the following derivations can be carried out in either reference frame and yield the same results.

According to the conservation of mass, the mass flux ($\dot{m}' = \frac{\dot{m}}{A} = \frac{\rho u A}{A} = \rho u$) into the control volume ($\rho_0(U_s - u_0)$) must be equivalent to the mass flux out of the

[1]This relationship is valid as long as the shock velocity is much slower than the speed of light [2], which is generally true.

control volume ($\rho_1(U_s - u_1)$) plus the time rate of change of mass within the control volume per unit area. [2] The assumption that the shock is in steady flow is appropriate in most cases, since shock waves travel at a constant velocity, with a constant change in pressure across the wave front [1]. The conservation of mass results in Equation 1.1, which relates initial and final densities ρ_0 and ρ_1, as well as initial and final particle velocities u_0 and u_1 and the shock velocity, U_s. If the material being shocked begins at rest ($u_0 = 0$), Equation 1.1 simplifies to Equation 1.2. This relationship easily relates the densities of material flowing into and out of the shock front and leads to practical simplifications further on.

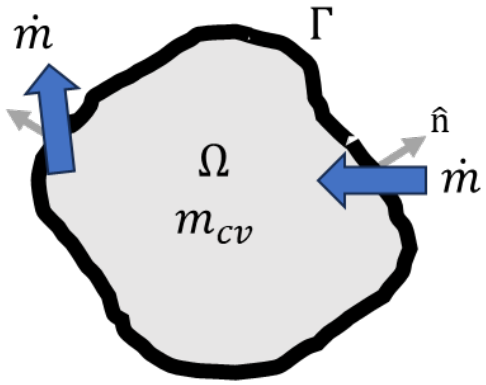

Figure 1.2: Control volume: conservation of mass.

[2] See list of symbols in Appendix A.

$$\frac{d}{dt}\int_{\Omega}\rho d\Omega = \int_{\Gamma} -\hat{n}_i(\rho u_i)d\Gamma$$
$$\frac{dm_{cv}}{dt} = \dot{m}_{in} - \dot{m}_{out}$$
$$0 = \rho_0(U_s - u_0) - \rho_1(U_s - u_1)$$
$$\rho_1(U_s - u_1) = \rho_0(U_s - u_0) \tag{1.1}$$

$$If\ u_0 = 0:$$
$$\rho_1(U_s - u_1) = \rho_0 U_s \tag{1.2}$$

The conservation of momentum suggests that the sum of forces applied to a body equal the time rate of change in momentum of the body. In a control volume, the linear momentum flux ($\dot{p_i'} = \frac{\hat{n}_k \dot{m}_k u_i}{A} = \frac{A\hat{n}_k(\rho u_k)u_i}{A} = \hat{n}_k(\rho u_k)u_i$) needs to be considered as well. When applied to the one-dimensional control volume containing the shock, the control volume neither accumulates mass nor accelerates, so the momentum contained in the control volume is constant; however, there is a significant change in the momentum flow into the system and the momentum flowing out. This is counteracted (on a per unit area basis) by the change in stress across the control volume. By substituting Equation 1.1 into Equation 1.3, Equation 1.4 can be derived. Finally, if the material being shocked begins at rest and at zero pressure, the equations reduce to Equation 1.5.

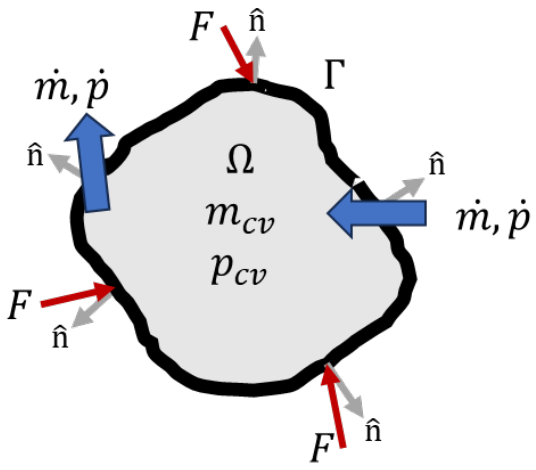

Figure 1.3: Control volume: conservation of linear momentum.

$$\frac{d}{dt}\int_{\Omega}\rho u_i d\Omega = \int_{\Gamma}\sigma_{ij}\hat{n}_j d\Gamma + \int_{\Gamma} -\hat{n}_k(\rho u_k)u_i d\Gamma$$

$$\frac{dp_{cv}}{dt} = \sum F - \dot{p}_{out} + \dot{p}_{in} = 0$$

$$0 = \Sigma P - \dot{p}'_{out} + \dot{p}'_{in}$$

$$P_1 - P_0 = \dot{m}_1 u_{out} - \dot{m}_0 u_{in}$$

$$P_1 - P_0 = \rho_1(U_s - u_1)(u_1 - U_s) - \rho_0(U_s - u_0)(u_0 - U_s) \tag{1.3}$$

$$P_1 - P_0 = \rho_0(U_s - u_0)(u_1 - U_s) - \rho_0(U_s - u_0)(u_0 - U_s)$$

$$P_1 - P_0 = \rho_0(U_s - u_0)(u_1 - u_0) \tag{1.4}$$

$$P_1 = \rho_0 U_s u_1 \tag{1.5}$$

Finally, to carry out impedance matching, it must be understood that when an interface between two materials is at equilibrium the particle velocities as well as the stresses on either side of the interface must be equivalent. For cases where it is okay to assume that the materials at play are approximately hydrodynamic—that is to say that the pressure is large enough to render the yield strengths of the materials insignificant—that stress and pressure are one and the same, so only the

pressure must be equal on either side of an interface for equilibrium to be achieved. When considering that the stress must be equivalent on either side of an interface in equilibrium, it would be most accurate to state that the traction on either side of the interface must be equal and opposite, as seen in Equation 1.6, wherein three components of the stress tensor must be equal. Traction (t_i) is the portion of a stress tensor applied to a particular surface (defined by it's normal vector) and is effectively the force per unit area on that surface, as defined by the dot product of the stress tensor with the unit normal vector. Since impedance matching is only applicable for uniaxial strain, all shear strains will be zero. In the vast majority of materials, zero elastic shear strain means zero shear stress. This could be contradicted by an unusual material such as a composite with an anisotropic lay-up, but is rarely a concern.

$$\begin{gathered}
\sigma_{ij}^{(1)}\hat{n}_j^{(1)} = t_i^{(1)} = -t_i^{(2)} = -\sigma_{ik}^{(2)}\hat{n}_k^{(2)} \\
\hat{n}_i^{(1)} = \begin{bmatrix} 1 \\ 0 \\ 0 \end{bmatrix}, \hat{n}_k^{(2)} = \begin{bmatrix} -1 \\ 0 \\ 0 \end{bmatrix} \\
\begin{bmatrix} \sigma_{11}^{(1)} \\ \sigma_{12}^{(1)} \\ \sigma_{13}^{(1)} \end{bmatrix} = \begin{bmatrix} \sigma_{11}^{(2)} \\ \sigma_{12}^{(2)} \\ \sigma_{13}^{(2)} \end{bmatrix}
\end{gathered} \tag{1.6}$$

Finally, the method of impedance matching can be defined. This method is applicable to any uniaxial shock event, but here, only a two material shock event will be discussed as this is the relevant case for the available experimental data.

First, the material parameters should be established as known values: ρ_A, ρ_B, C_A, C_B, s_A, and s_B, where material A is impacting material B at initial velocity u_0. To determine the first interaction, the particle velocity (u_1) and pressure (P_1),

the shocks moving into each material should be considered.The shock traveling into material B (the target) will increase particle velocity from 0 to u_1 while increasing pressure from 0 to P_1. The shock traveling into material A (the projectile) will decrease particle velocity from u_0 to u_1 (in the flyer's initial reference frame, the particle velocity increases from 0 to $u_1 - u_0$) and increase pressure from 0 to P_1. Since P_1 and u_1 need to match on either side of the interface, the following relations can be set up:

$$\begin{aligned} P_1 &= P_1^A = P_1^B \\ P_1 &= \rho_A(U_s)(u_1 - u_0) = \rho_B(U_s - 0)(u_1 - 0) \end{aligned} \tag{1.7}$$

Most materials have been observed to follow a linear $U_s - u_p$ behavior[5]. While this relationship is evident experimentally, it is also a Taylor series expansion, so a quadratic term could be included as well. The linear form is sufficient for most materials over a limited range of pressures.

$$U_s = C_0 + su_p \tag{1.8}$$

Substituting Equation 1.8 into Equation 1.7 results in the following:

$$P_1 = \rho_A(C_A + s_A(u_0 - u_1))(u_0 - u_1) = \rho_B(C_B + s_B u_1)u_1 \tag{1.9}$$

From here, the final unknown, particle velocity, u_1, can be determined analytically (using the quadratic formula) or numerically. Finally, the shock wave velocity and pressure can be determined by plugging the known value of u_1 back into Equations 1.8 and 1.9.

The next interaction of interest is the reflection of the shock wave off the rear free-surface of the target. When the wave reaches a free-surface, the traction on the interface must be zero, since there is nothing to provide an equal and opposite

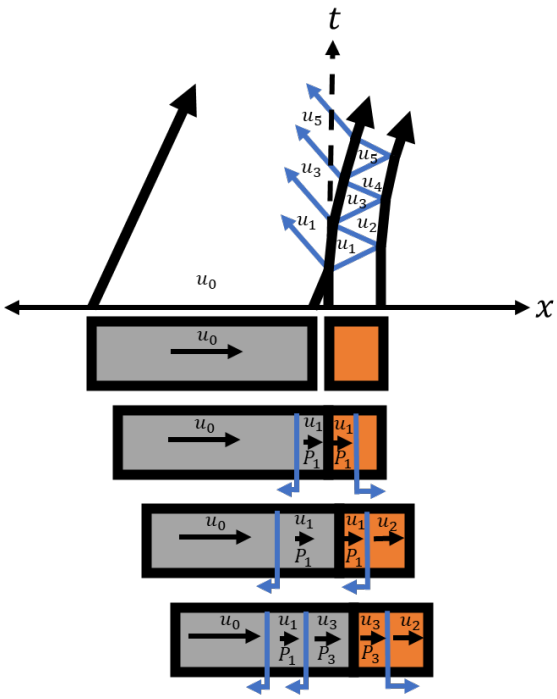

Figure 1.4: Impedance matching: reverb X-T diagram.

reaction. Therefore, the pressure (or the stress where applicable) must release to zero. While the resulting pressure is known ($P_2 = 0$), the resulting particle velocity (u_2) is of interest, since this is the velocity that can be measured experimentally. A new conservation of momentum equation will be used to determine this velocity, but the equation will be modified such that the material accelerates forward (an increase in velocity) into the free space so that the pressure decreases to zero, resulting in Equation 1.10. Substitution of Equation 1.9 into 1.10 results in 1.11. Here, the application of Equation 1.9 assumes that the material releases along the Hugoniot rather than the isentrope. This assumption leads to a small amount of error [1].

$$P_1 - 0 = \rho_B U_s (u_2 - u_1) \tag{1.10}$$

$$\rho_B (C_B + s_B u_1) u_1 = \rho_B (C_B + s_B (u_2 - u_1))(u_2 - u_1) \tag{1.11}$$

This algebraic expression is solved if $u_1 = u_2 - u_1$, resulting in the convenient relationship in Equation 1.12. A Galilean transformation ($u' = u_0 - u$) to a

reference frame moving at the original velocity of the projectile transforms this into the velocity change seen by the flyer, since this is the relevant velocity for the equation of state information relevant to the projectile. Finally, the measured velocity in the stationary observer's reference frame (u_2) can be related to the velocity difference seen in the projectile's initial reference frame, u_1'.

$$u_2 = 2u_1 \tag{1.12}$$

$$u_2 = 2(u_0 - u_1')$$

$$u_1' = u_0 - \frac{u_2}{2} \tag{1.13}$$

The left-going wave will reflect off the impact interface, resulting in values for u_3 and P_3, which can be determined in a similar derivation to Equation 1.9. Then, in a similar derivation to Equation 1.12, u_4 can be determined to be:

$$u_4 = 2u_3 - u_2 \tag{1.14}$$

$$u_3' = u_0 - \frac{u_4 + u_2}{2} \tag{1.15}$$

In a reverb experiment, u_2, u_4, and so on can be measured, but u_1', P_1; u_3', P_3; and so on represent important information for determining the equation of state of the flyer material (the goal of the experiment). Using the relationships here (Equations 1.13 and 1.15), this data can easily be accessed. Unfortunately, these simple relationships become inaccurate when the yield strength of the target material is significant relative to the pressure of the shock wave.

1.1.1 Elastic-Plastic Impedance Matching

Impedance matching of materials that remain elastic is even simpler than materials that behave hydrodynamically (as discussed above) since elastic waves

travel at a constant speed—C_L ; therefore, the $\sigma_{11} - u_p$[3] relationship is linear[5]:

$$C_L = \sqrt{\frac{M}{\rho}} \tag{1.16}$$

$$\sigma_{11} = \rho_0 C_L u_p \tag{1.17}$$

This relationship makes the derivations above relevant for purely elastic materials, and Equations 1.12 and 1.14 are still accurate. However, the complexities arise when the target material's yield strength is slightly exceeded. In an elastic-plastic impedance match, the stress normal to the interface must be equivalent on either side. It is helpful to decompose the stress tensor into a symmetric and deviatoric part:

$$\sigma_{ij} = P\delta_{ij} + s_{ij} \tag{1.18}$$

$$\sigma_{11} = P + s_{11} \tag{1.19}$$

This decomposition is convenient as the hydrostatic (spherical) term can be calculated with Equation 1.5, and the deviatoric term can be calculated with a modified Equation 1.17. This decomposition will also simplify determining the von Mises stress, which is independent of pressure. See derivation in Appendix B, which results in Equation 1.20.

$$\sigma_{11} = P \pm \frac{2}{3}\sigma_{vm} \tag{1.20}$$

$$|s_{11}| = \frac{2}{3}\sigma_{vm} \tag{1.21}$$

[3]Where the unit vector e_1 points in the direction that the shock travels in, and σ_{11} represents the component of the stress tensor in the e_1e_1 direction, rather than the eleventh stress state.

Substituting Equations 1.17 and 1.5 into equation 1.20 results in a form that is easier to implement numerically.

$$\rho_0 C_L u_p = \rho_0 U_s u_p + s_{11} \tag{1.22}$$

$$\rho_0 C_L^{dev} u_p = s_{11} \tag{1.23}$$

$$C_L^{dev} \doteq C_L - C_0 \tag{1.24}$$

C_L^{dev} has no physical meaning and is only a numerical artifact, which cannot be measured experimentally. As such, there could be alternate definitions such as $C_L - U_s$ or $C_L - C_B$, which depend on the constitutive relationship and should give similar results.

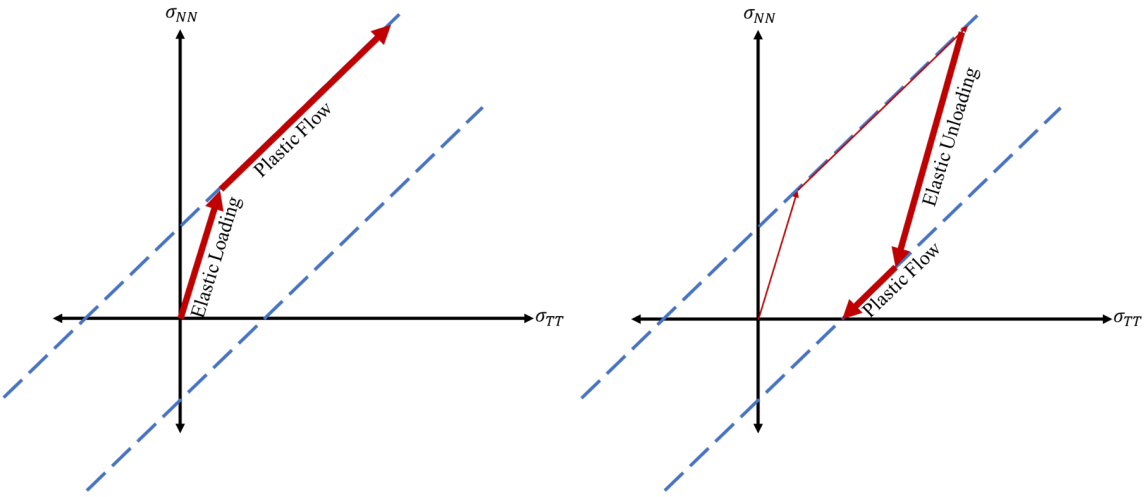

Figure 1.5: Elastic-plastic shock loading and unloading with von Mises yield surface (Dashed Lines)

To determine a stress-velocity pair upon impact, the same method used from impedance matching without strength can be used, but the first step is to assume that the material remains elastic all the way to the end state, then if the equivalent stress at that endpoint exceeds the yield strength of the material, set $s_{11} = \pm\frac{2}{3}\sigma_y$, and resolve the pressure term from there. This process is easy enough for

determining the stress upon impact of a purely elastic or a purely inelastic material with an elastic-plastic material, but if both materials are elastic-plastic, stress might have to be evaluated for the various situations where each material does or does not yield. There could be multiple solutions to an implicit solver. Another issue that arises is how to deal with a release (unloading). Upon release into free space, the combined stress on the interface with free space must be zero in the direction of the free-surface (σ_{11}); however, it would be too easy to assume that the pressure and deviatoric parts are both zero. Instead, the material will release elastically from one side of the von Mises yield surface, past zero, and potentially all the way to the other side—as illustrated in Figure 1.5. However, if the material only slightly yielded upon initial loading, the release may be completely elastic. These complexities make implicit impedance matching difficult, and the problem becomes easier to solve explicitly, where the deviatoric contribution to stress is calculated by integrating $ds_{11} = \rho_0(C_L - C_0)du_p$. Then, determine if the von Mises equivalent stress exceeds the yield strength; if so, use a radial return method to determine the stress state. Due to the uniaxial strain state, a very simple radial return method can be used:

$$if|s_{11}^{(0)}| > \frac{2}{3}\sigma_y : \tag{1.25}$$

$$s_{11} = sign(s_{11}^{(0)})\frac{2}{3}\sigma_y \tag{1.26}$$

One significant assumption incorporated in this method is that the shock wave remains a single discrete step. In reality, the elastic precursor travels at the velocity C_L, whereas the shock wave travels at U_s. In shock waves of moderate pressures, C_L is greater than U_s; therefore, the elastic wave will race ahead of the shock wave. This creates a significant amount of complexity as then the interactions between a reflected elastic wave with the shock wave need to be resolved. To reduce the complexity of this method, only the final shock stress will be considered. This is

a prudent assumption as no experimental measurements used here were able to observe a distinct elastic precursor; however, this approximation may need to be reconsidered to achieve precise calculations.

This method adds a significant level of complexity to the simple hydrodynamic method of impedance matching; nevertheless, for shock waves that only slightly exceed the yield strength of a material, this method presents a significant improvement in accuracy, compared to the hydrodynamic assumption. A number of assumptions have been taken in developing this method to limit complexity, while producing physical results. An example of elastic-plastic impedance matching will be presented in Section 1.2.2 to determine the material properties of UV resin.

1.2 UV Resin Reverb

The target used for the UV resin reverb experiment consisted of 304 stainless steel, 2024 aluminum, and 110 copper. The relevant equation of state parameters for these materials can be found in Table 1.1. These materials were chosen to present the UV resin with a variety of points of comparison. Aluminum presents a lower impedance, while the copper and steel have similar impedances but significantly different yield behaviors. Copper has a lower strength than steel, but the significant ductility of copper may expose interesting sensitivities of the strength behavior of the UV resin. All three metals have been well-studied and have published equation of state and strength models. Yet, it is worth considering that these equation of state models are based on data ranging from 5 to 200 GPa [1], which may be greater than the pressures achieved in these experiments; unfortunately, to know if the experiments reached these pressures, an accurate model of the material of interest would be required. Since the purpose of these experiments is to determine a model for the UV resin, it must be assumed that the

published models for the target materials are applicable and whether this was a good assumption can be reassessed once a model has been determined.

Table 1.1: UV resin reverb target material parameters [5].

Material	ρ_0 $\frac{kg}{m^3}$	C_0 $\frac{m}{s}$	s_1	c_v $\frac{J}{kg-K}$	γ_0
2024 aluminum	2700	5350	1.34	890	2.0
304 stainless steel	7900	4570	1.49	440	2.2
110 copper	8960	3940	1.49	400	2.0

Four experiments (discussed in [6]) were carried out at projectile velocities: 503, 365, 141, and 89 $\frac{m}{s}$. These velocities were chosen to probe the material at the pressure range of interest; unfortunately, measurements of the 141 and 89 $\frac{m}{s}$ shots were not clear enough to be useful. Figure 1.6 shows PDV (photon Doppler velocimetry) measurements from these experiments. The measured Hugoniot and first release plateau velocities (u_{p2} and u_{p4} respectively) are shown for the six experiments in Table 1.2. These measurements will be the basis for the impedance matching method.

Table 1.2: UV resin reverb experimental measurements: plateau velocities.

Material	Projectile Velocity u_0 m/s	Hugoniot Plateau u_2 m/s	First Release Plateau u_4 m/s
Aluminum	365	125.9	196.5
Copper	365	59.8	105.7
Steel	365	53.8	105.7
Aluminum	503	185.4	286.1
Copper	503	90.7	155.8
Steel	503	78.7	140.2

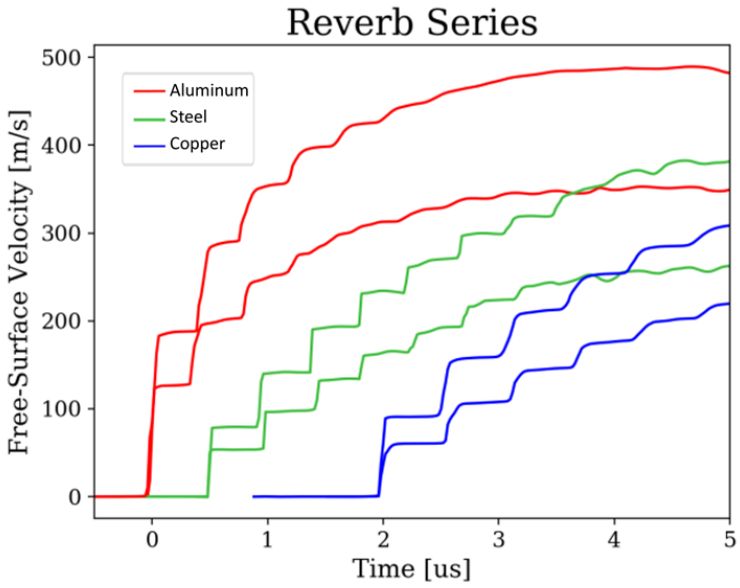

Figure 1.6: UV resin reverb experimental results [6] at projectile velocities of $503\frac{m}{s}$ and $365\frac{m}{s}$ for three target materials

1.2.1 Impedance Matching

The method of impedance matching can be used to calculate equation of state information from these plateaus. Assuming that all materials are hydrodynamic makes this process straightforward. This assumption leads to Equation 1.12 and Equation 1.14, wherein the particle velocity upon impact can be determined, as well as the particle velocity upon reflection of the first release wave. From there, Equation 1.4 can be used to determine the pressure of these interactions based on the known model of the target material. From these equations, the pressure and particle velocity of a Hugoniot state (state 1) and a release state (state 3) can be determined. This data is presented in table 1.3.

Finally, a set of $U_s - u_p$ data can be determined by solving Equation 1.4 for U_s, while using the measured density of UV resin. This data can be seen in Figure 1.7, and a linear fit can be performed to determine a Hugoniot slope (s) and

Table 1.3: UV resin reverb: impedance matched pressures and particle velocities.

Target Material	u_0 m/s	u_1 m/s	P_1 MPa	u_3 m/s	P_3 MPa
Aluminum	365	301.8	927.2	202.7	524
Copper	365	334.8	1077	281.8	816
Steel	365	338.2	975	289.9	783
Aluminum	503	409.5	1326	265.3	741
Copper	503	457.6	1632	379.0	1184
Steel	503	463.4	1447	392.9	1127

intercept (C_0). The resulting parameters as well as the measured density are presented in Table 1.4.

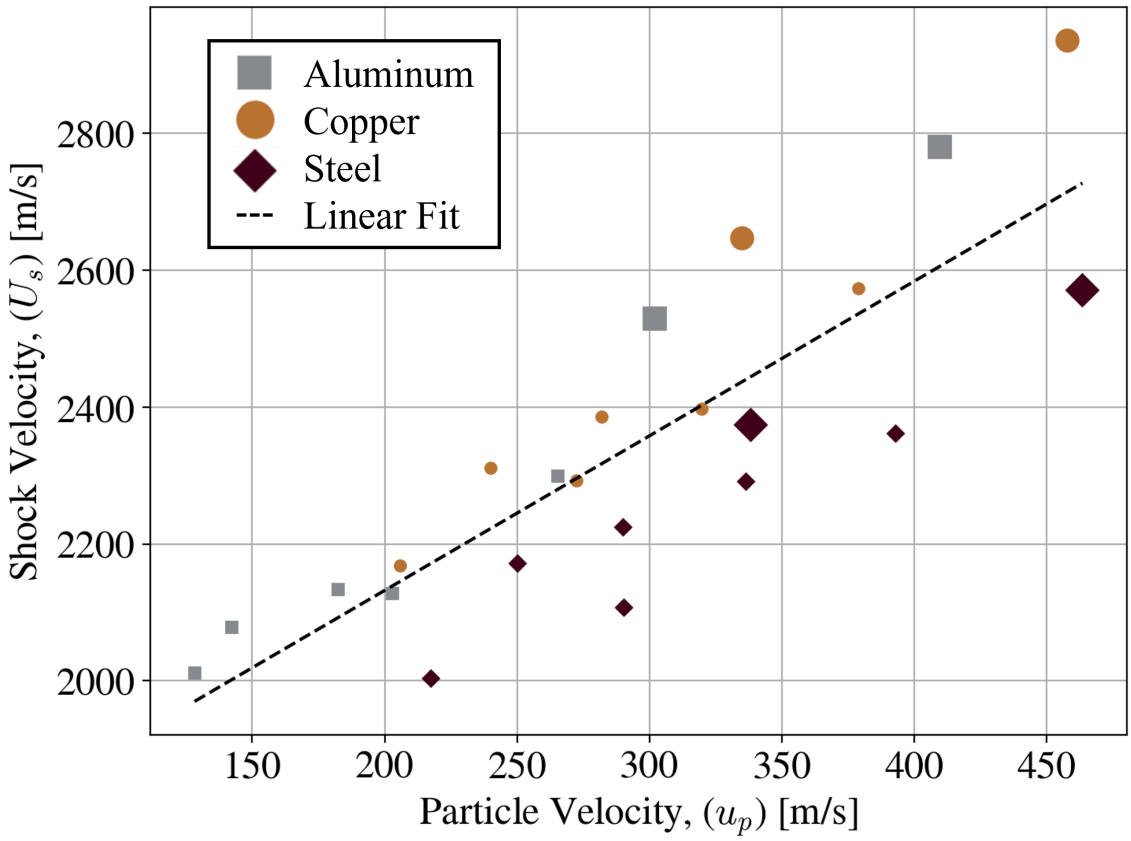

Figure 1.7: UV resin: impedance matched $Us - up$ data. Large markers represent Hugoniot states of the UV resin; small markers represent release states.

Table 1.4: UV resin material parameters from hydrodynamic impedance matching.

Density ρ_0 $\frac{kg}{m^3}$	Hugoniot Intercept C_0 $\frac{m}{s}$	Hugoniot Slope s
1214 [6]	1680	2.26

A trend starts to emerge in Figure 1.7 where the calculated shock velocities derived from measurements of the steel targets are lower than those derived from the copper and aluminum target measurements. There can be two theories to determine the source of this correlation. First, since the equations of state of the targets are derived from experiments that all exceed the pressures predicted in table 1.3, these material models are not valid at these low pressures. This may be true, but without more information about these materials at low pressures, it would be difficult to find a way to verify this theory or mitigate potential source of error. However, the second theory explaining this difference may be rectifiable: perhaps the elasticity of the targets must be considered. This theory is somewhat confirmed by running the calculated parameters through a set of hydrocode simulations where the targets are modeled with strength. The results of these simulations (dashed lines) compared to the experimental measurements (solid lines) are shown in Figure 1.8, and can be seen to fail to replicate the measured velocity traces. Furthermore, all simulated plateaus have lower velocities than those measured, meaning that the remaining error is not evenly distributed about zero, suggesting that the parameters determined via impedance matching do not form a good model.

1.2.2 Elastic-Plastic Impedance Matching

The elastic-plastic impedance matching method introduces significant complexity to determining a material model. Not only is determining if a material yields an increase in complexity, but whether or not the target material yields

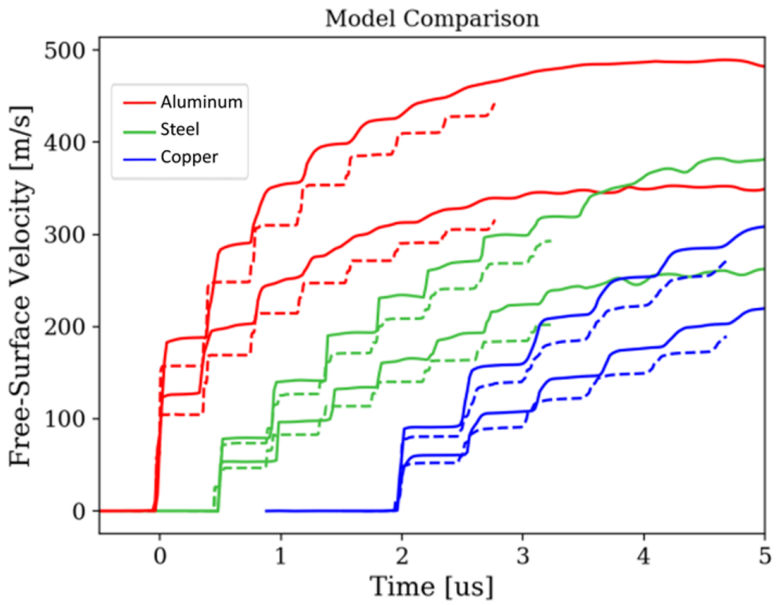

Figure 1.8: Simulation with calculated parameters (dashed) compared to experimental measurements (solid).

depends on the unknown material model. This dilemma makes determining $U_s - u_p$ data not straightforward and will not result in a linear fit like Figure 1.7. Instead, a conventional optimization method will be set up to iteratively solve for the u_2 values with a given set of parameters and compared to the measurements. The solver will be MATLAB's fminsearch function, which requires an initial guess for C_0 and s (these will be pulled from the hydrodynamic impedance matching results). The objective function for the solver to minimize is the sum squared of the errors for all six Hugoniot plateaus.

The equation of state parameters for the target materials in Table 1.4 were reused, with the addition of the elastic-plastic parameters shown in Table 1.5. From these parameters, the longitudinal elastic sound speed can be derived with Equation 1.16.

Figure C.1 shows the results of the elastic-plastic impedance matching with the UV resin equation of state derived from the hydrodynamic linear fit. When the

Table 1.5: UV resin reverb target materials: elastic-plastic parameters.

Material	Young's Modulus E GPa	Poisson's Ratio ν	Yield Strength σ_Y MPa
2024 aluminum[7]	73	0.33	76
304 stainless steel[8]	200	0.28	215
110 copper[9]	110	0.343	90

experimental values are compared to the theoretical u_{p2} values resulting from this impedance match, it is clear to see that the theoretical values fall short of the measurements in all six cases, which mirrors the simulations in Figure 1.8. Error can be quantified as the difference between these values, and for these parameters (taken from Table 1.4), the root-mean-squared-error is 12.8 m/s.

Once the optimization is set up in MATLAB, the optimization can be run in around two minutes on a single processor. The optimized parameters can be seen in Table 1.6, and the final root-mean-squared-error is 1.4 m/s (much reduced from the initial parameter set). The impedance matches of the final UV resin Hugoniot can be seen in Figure C.2. The remaining errors are approximately evenly distributed about zero, whereas the initial errors can be seen to be strongly skewed.

Table 1.6: UV resin material parameters from optimized elastic-plastic impedance matching.

Density ρ_0 $\frac{kg}{m^3}$	Hugoniot Intercept C_0 $\frac{m}{s}$	Hugoniot Slope s
1214 [6]	2457	1.23

1.3 Final Remarks on Impedance Matching

The values converged upon by the elastic-plastic impedance matching code are significantly different than the values derived from the hydrodynamic impedance matching method; in fact, the Hugoniot intercept is 45% greater according to these results. These values are much better estimates of the true Hugoniot, but a complete material model has not yet been developed. The values derived so far are understood to directly determine the values measured experimentally; but determining the hardening modulus or the strain-rate sensitivity of the UV resin is a more difficult task as it is not well understood how these parameter affects the result of a reverb experiment. To improve upon the model, an optimization could be set up similar to the elastic-plastic impedance matching method, where a complex method is run in a hydrocode and simulation results are compared to experimental data. However, as the number of model parameters increases, the effectiveness and efficiency of conventional methods of optimization such as gradient descent or the simplex method (used by Matlab's $fminsearch$ function [10]) decreases due to the increased complexity of the input and output spaces. Furthermore, conventional methods such as these have inevitable bias built in, which affects the optimal solution. In the elastic-plastic optimization routine, the combination of six error values into one heuristic unfairly biases the higher velocity data because the margins are greater.

BIBLIOGRAPHY

[1] Jerry W. Forbes. *Shock Wave Compression of Condensed Matter*. Springer, 2012.

[2] Thomas A. Moore. *A General Relativity Workbook*. University Science Books, 2013.

[3] Galileo Galilei. *Dialogue Concerning the Two Chief World Systems*. 1632.

[4] Isaac Newton. *Principia*. 1687.

[5] Marc A. Meyers. *Dynamic Behavior of Materials*. Wiley-Interscience, New York, 1994.

[6] Jack D. Borg. Additively manufactured granular and binder metamaterial's response to shock. Master's thesis, Marquette University, Milwaukee, WI, December 2022.

[7] Aluminum 2024-t4; 2024-t351. https://www.matweb.com/search/DataSheet.aspx?MatGUID=67d8cd7c00a04ba29b618484f7ff7524.

[8] 304 stainless steel. https://www.matweb.com/search/datasheet.aspx?MatGUID=abc4415b0f8b490387e3c922237098da&ckck=1.

[9] Copper, cu; annealed. https://matweb.com/search/DataSheet.aspx?MatGUID=9aebe83845c04c1db5126fada6f76f7e&ckck=1.

[10] fminsearch. https://www.mathworks.com/help/matlab/ref/fminsearch.html#bvadxhn-12.

[11] Ted Belytschko, Wing Kam Liu, Brian Moran, and Khalil I. Elkhodary. *Nonlinear Finite Elements for Continua and Structures*. Wiley, Chichester, West Sussex, United Kingdon, second edition, 2014.

APPENDIX A

LIST OF SYMBOLS

Table A.1: List of Symbols

Symbol	Description	Unit
U, U_s	Shock Wave Velocity	$\frac{m}{s}$
$u, u_p, u_\#$	Particle Velocity[1,2]	$\frac{m}{s}$
$\rho, \rho_\#$	Density	$\frac{kg}{m^3}$
$P, P_\#$	Pressure	$\frac{N}{m^2}, Pa$
σ_{ij}	Stress Tensor[3]	Pa
s_{ij}	Stress Deviator	Pa
$\bar{\sigma}$	Von-mises Equivalent Stress	Pa
ε_{ij}	Strain Tensor	
$\bar{\varepsilon}$	Equivalent Plastic Strain (EQPS)	
$\dot{\varepsilon}$	Strain-rate	$\frac{1}{s}$
t_i	Traction ($\sigma_{ij}\hat{n}_j$)	Pa
C_{ijkl}	Constitutive Modulus Tensor	Pa
E	Young's Modulus[4]	Pa
M	P-Wave Modulus[5]	Pa
G, μ	Shear Modulus	Pa
K	Bulk Modulus	Pa
λ	Lame's Constant	Pa
$\dot{m}$	Mass Flow Rate	$\frac{kg}{s}$
$\dot{m}'_i$	Mass Flux	$\frac{kg}{m^2-s}$
p_i	Linear Momentum ($\frac{dT}{d\dot{q}_i}$)	$\frac{J}{m/s}, \frac{kg-m}{s}$
$\dot{p}'_i$	Momentum Flux	$\frac{kg-m}{m^2-s^2}, \frac{N}{m^2}, Pa$
CV	Control Volume[6]	
Ω	The Interior of a Control Volume	m^3
Γ	The Surface of a control Volume	m^2
A	Area	m^2
$A_i, A\hat{n}_i$	Area Vector	m^2
$\hat{n}_i$	Unit Normal Vector	
$\|\|x\|\|$	Euclidean Length of a Vector or Tensor	
δ_{ij}	Kronecker Delta ($1(i=j)$))	

Table A.2: List of Symbols: Mie-Grueneisen Equation of State

Symbol	Description	Unit
C_0	Hugoniot Intercept	$\frac{m}{s}$
s	Hugoniot Slope	
γ_0	Grueneisen Coefficient	
c_v	Specific Heat	$\frac{J}{kg-K}$
ρ_0	Initial Density	$\frac{kg}{m^3}$
P_H	Hugoniot Pressure	Pa
e	Energy	J
e_H	Hugoniot Energy	J

Table A.3: List of Symbols: Johnson-Cook Strength Model

Symbol	Description	Unit
A	Initial Yield Strength	$\frac{m}{s}$
B	Strain-Hardening Coefficient	Pa
n	Strain-Hardening Exponent	
C	Strain-rate Sensitivity	
m	Thermal Softening Exponent	
T	Temperature	K
T_{melt}	Melt/glass-transition Temperature	K
T_0	Reference (room) Temperature	K

APPENDIX B

ELASTIC-PLASTIC IMPEDANCE MATCHING: ADDITIONAL DERIVATIONS

$$\sigma_{ij} = C_{ijkl}\varepsilon_{kl} \tag{B.1}$$

$$C_{ijkl} = \lambda\delta_{ij}\delta_{km} + \mu(\delta_{ik}\delta_{jm} + \delta_{im}\delta_{jk})[11] \tag{B.2}$$

$$\epsilon_{ij} = \begin{bmatrix} \varepsilon & 0 & 0 \\ 0 & 0 & 0 \\ 0 & 0 & 0 \end{bmatrix} \tag{B.3}$$

$$\sigma_{ij} = C_{ij11}\varepsilon_{11} \tag{B.4}$$

$$C_{ijxx} = \lambda\delta_{ij}\delta_{xx} + \mu(\delta_{ix}\delta_{jx} + \delta_{ix}\delta_{jx}) \tag{B.5}$$

$$= \lambda\delta_{ij} + 2\mu(\delta_{ix}\delta_{jx}) \tag{B.6}$$

$$\sigma_{ij} = \varepsilon(\lambda\delta_{ij} + 2\mu(\delta_{ix}\delta_{jx})) \tag{B.7}$$

$$\sigma_{xx} = \varepsilon(\lambda + 2\mu) = \varepsilon_{xx}M \tag{B.8}$$

$$\sigma_{yy} = \sigma_{zz} = \varepsilon\lambda \tag{B.9}$$

$$\sigma_{yz} = \sigma_{xz} = \sigma_{xy} = 0 \tag{B.10}$$

$$\sigma_m = \frac{\sigma_{kk}}{3} \tag{B.11}$$

$$= \varepsilon\frac{1}{3}(3\lambda + 2\mu) \tag{B.12}$$

$$= \varepsilon(\lambda + \frac{2}{3}\mu) = \varepsilon_{xx}K \tag{B.13}$$

$$\sigma_{ij} = \sigma_m\delta_{ij} + s_{ij} \tag{B.14}$$

$$s_{xx} = \frac{4}{3}\mu\varepsilon \tag{B.15}$$

$$s_{yy} = s_{zz} = -\frac{2}{3}\mu\varepsilon \tag{B.16}$$

$$\bar{\sigma} = (\frac{3}{2}s_{ij}s_{ij})^{\frac{1}{2}}[11] \tag{B.17}$$

$$s_{ij}s_{ij} = (\frac{4}{3}\mu\varepsilon)^2 + 2(-\frac{2}{3}\mu\varepsilon)^2 \tag{B.18}$$

$$= \frac{24}{9}\mu^2\varepsilon^2 = \frac{8}{3}\mu^2\varepsilon^2 \tag{B.19}$$

$$\bar{\sigma} = (\frac{3}{2}\frac{8}{3}\mu^2\varepsilon^2)^{\frac{1}{2}} = (4\mu^2\varepsilon^2)^{\frac{1}{2}} \tag{B.20}$$

$$= 2\mu|\varepsilon| \tag{B.21}$$

$$s_{xx} = \pm\frac{2}{3}\bar{\sigma} \tag{B.22}$$

$$s_{yy} = s_{zz} = \mp\frac{1}{3}\bar{\sigma} \tag{B.23}$$

APPENDIX C

ELASTIC-PLASTIC IMPEDANCE MATCHING RESULTS

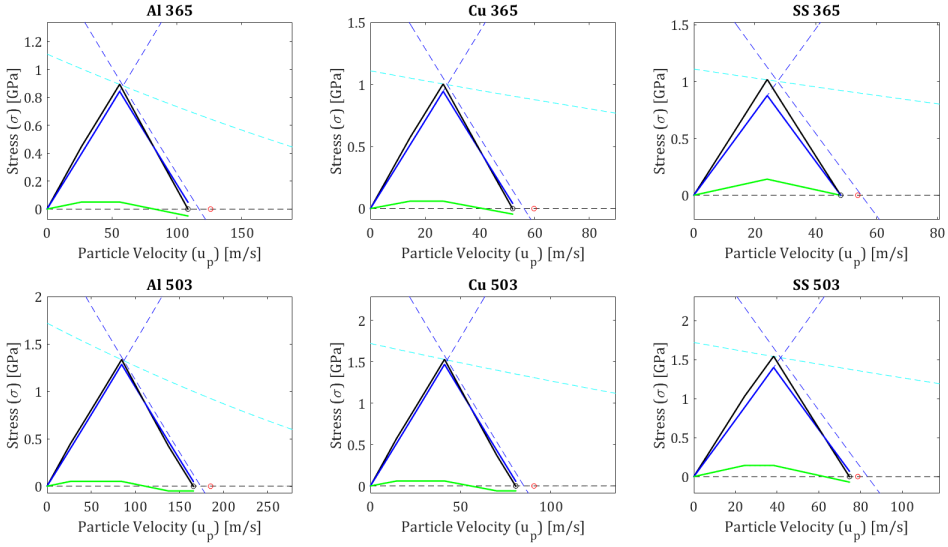

Figure C.1: UV resin elastic-plastic impedance match with EOS parameters from hydrodynamic impedance match

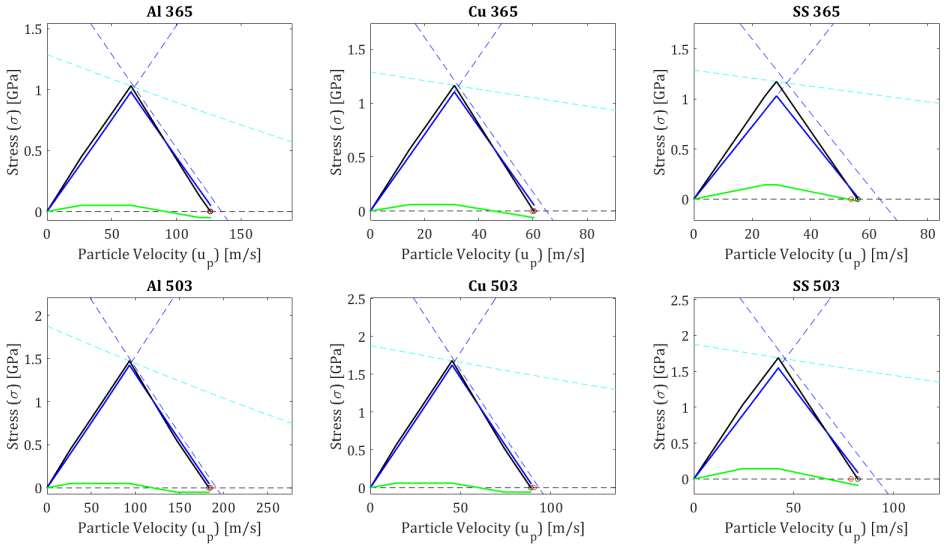

Figure C.2: UV resin elastic-plastic impedance match with optimized parameters

In these figures, the hydrodynamic impedance match is shown with dashed lines. The UV resin EOS is colored cyan, while the target metal is blue. The elastic-plastic impedance match is styled with solid lines representing the stress states achieved in the target metal. The stress (σ_{11}) is colored black, and broken into mean and deviatoric (s_{11}) components, colored blue and green respectively. The calculated velocity (u_1) is displayed as a black circle on the x-axis, while the corresponding measurement is displayed as a red circle.